Advances in Difference Equations
a SpringerOpen Journal

RESEARCH Open Access

Curved beam elasticity theory based on the displacement function method using a finite difference scheme

Wankui Bu[1*] and Hui Xu[1]

*Correspondence:
317903244@qq.com
[1]College of Urban Construction, Heze University, Heze City, China

Abstract

A displacement function suitable for plane curved beam in polar coordinates is introduced, and a partial differential governing equation of plane curved beam is obtained by theoretical analysis. Then, the formulation of displacement components and stress components is expressed by the displacement function. On this basis, a finite difference scheme of the partial differential governing equation, displacement components, and stress components of an elastic body in polar coordinates is presented. Finally, the finite difference equations of theoretical formulation are applied to analyze the stress distribution of curved rock, which will provide scientific basis and reference for coal mining engineering.

Keywords: Displacement function; Elastic theory of curved beam; Finite difference method; Curved rock

1 Introduction

The stress function method has been successfully applied to solve curved beam problems in the theory of elasticity, such as the Lame solution of the ring or cylinder subjected to the uniform pressure, the Guo solution of the curved beam bearing bending moment [1–7], the Kirs solution of the stress concentration at the edge of circular hole, the Mitchell solution and the Gris solution and Li solution for the wedge body bearing surface force, and the Flamant solution of the semi-planar body subjected to concentrated force on the boundary [8–15]. The application of the stress function method has achieved certain results. The stress function can be obtained by solving the compatible equation for the axisymmetric problem or the simple non-axisymmetric problem [16–19]; however, the boundary condition can only be in terms of loading conditions. When the boundary restraint is in terms of radial or circumferential displacement/strain conditions, the stress function method cannot obtain satisfactory solution. On the other hand, the direct displacement parameters method involves finding two displacement parameters (radial displacement and circumferential displacement) from two partial differential equilibrium equations. However, it is very difficult to obtain two displacement parameters from two second order partial differential equations with variable coefficients, especially when the boundary conditions are in terms of mixed boundary with restrains and loadings. In practical applications, most practical problems with mixed boundary-value type are mainly accomplished by numeri-

cal calculation. The finite element method (FEM) and the finite difference method (FDM) are the major numerical methods. The FEM has been widely used in many fields, especially in the curve structure [20–23]. Gangan pointed out that the calculation error of a finite element will increase with the increase of flexure deformation [24]. It has been proved that the accuracy of FDM in stress analysis of structural members is higher than that of FEM [25, 26].

The displacement function suitable for curved beam with mixed boundary conditions in polar coordinates, which is defined in terms of radial and circumferential displacement components, is introduced in the present paper. Moreover, the partial differential governing equation of curved beam and the expression of displacement components and stress components are obtained in terms of displacement function. On this basis, the finite difference scheme of partial differential governing equation, displacement components, and stress components of elastic body in polar coordinates is presented. Finally, the finite difference equations of theoretical formulation are applied to analyze the stress distribution of curved rock.

2 Governing equations expressed by displacement components

With the elastic theory to a polar coordinate system (r,θ), the equilibrium equations for isotropic materials in terms of stress components σ_r, σ_θ, and $\tau_{r\theta}$ under plane strain conditions in the absence of body force are as follows:

$$\frac{\partial\sigma_r}{\partial r}+\frac{1}{r}\frac{\partial\tau_{r\theta}}{\partial\theta}+\frac{\sigma_r-\sigma_\theta}{r}=0, \tag{1a}$$

$$\frac{1}{r}\frac{\partial\sigma_\theta}{\partial\theta}+\frac{\partial\tau_{r\theta}}{\partial r}+\frac{2}{r}\tau_{r\theta}=0, \tag{1b}$$

$$\left(\frac{\partial^2}{\partial r^2}+\frac{1}{r}\frac{\partial}{\partial r}+\frac{1}{r^2}\frac{\partial^2}{\partial\theta^2}\right)(\sigma_r+\sigma_\theta)=0. \tag{1c}$$

For the plane strain, the stress components can be expressed as [1, 2]

$$\sigma_r=\frac{E(1-\mu)}{(1-2\mu)(1+\mu)}\left(\frac{\partial u_r}{\partial r}+\frac{\mu}{(1-\mu)r}\frac{\partial u_\theta}{\partial\theta}+\frac{\mu}{(1-\mu)r}u_r\right), \tag{2a}$$

$$\sigma_\theta=\frac{E(1-\mu)}{(1-2\mu)(1+\mu)}\left(\frac{\mu}{1-\mu}\frac{\partial u_r}{\partial r}+\frac{1}{r}\frac{\partial u_\theta}{\partial\theta}+\frac{1}{r}u_r\right), \tag{2b}$$

$$\tau_{r\theta}=\frac{E}{2(1+\mu)}\left(\frac{1}{r}\frac{\partial u_r}{\partial\theta}+\frac{\partial u_\theta}{\partial r}-\frac{u_\theta}{r}\right), \tag{2c}$$

where E and μ are the elastic modulus and Poisson's ratio of the material, respectively.

Taking the plane strain case as an example, the stress component expressions (2a)–(2c) are substituted into Eqs. (1a)–(1c), and the formulations are obtained as follows:

$$\frac{\partial^2u_r}{\partial r^2}+\frac{1}{2r(1-\mu)}\frac{\partial^2u_\theta}{\partial r\partial\theta}+\frac{(1-2\mu)}{2r^2(1-\mu)}\frac{\partial^2u_r}{\partial\theta^2}+\frac{1}{r}\frac{\partial u_r}{\partial r}-\frac{(3-4\mu)}{2r^2(1-\mu)}\frac{\partial u_\theta}{\partial\theta}-\frac{u_r}{r^2}=0, \tag{3a}$$

$$\begin{aligned}&\frac{(1-2\mu)}{2(1-\mu)}\frac{\partial^2u_\theta}{\partial r^2}+\frac{1}{2r(1-\mu)}\frac{\partial^2u_r}{\partial r\partial\theta}+\frac{1}{r^2}\frac{\partial^2u_\theta}{\partial\theta^2}+\frac{(1-2\mu)}{2r(1-\mu)}\frac{\partial u_\theta}{\partial r}\\&\quad+\frac{(3-4\mu)}{2r^2(1-\mu)}\frac{\partial u_r}{\partial\theta}-\frac{(1-2\mu)}{2r^2(1-\mu)}u_\theta=0,\end{aligned} \tag{3b}$$

$$\frac{\partial^3 u_r}{\partial r^3}+\frac{1}{r^3}\frac{\partial^3 u_\theta}{\partial \theta^3}+\frac{1}{r^2}\frac{\partial^3 u_r}{\partial r\partial\theta^2}+\frac{1}{r}\frac{\partial^3 u_\theta}{\partial r^2\partial\theta}+\frac{2}{r}\frac{\partial^2 u_r}{\partial r^2}+\frac{1}{r^3}\frac{\partial^2 u_r}{\partial\theta^2}-\frac{1}{r^2}\frac{\partial^2 u_\theta}{\partial r\partial\theta}-\frac{1}{r^2}\frac{\partial u_r}{\partial r}+\frac{1}{r^3}\frac{\partial u_\theta}{\partial\theta}+\frac{1}{r^3}u_r=0. \tag{3c}$$

Equations (3a) and (3b) are derived by r and θ, respectively, and the expressions of $\frac{\partial^3 u_r}{\partial r^3}$ and $\frac{\partial^3 u_\theta}{\partial\theta^3}$ are obtained.

$$\frac{\partial^3 u_r}{\partial r^3}=\frac{2}{r^2}\frac{\partial^2 u_\theta}{\partial r\partial\theta}-\frac{1}{2r(1-\mu)}\frac{\partial^3 u_\theta}{\partial r^2\partial\theta}+\frac{(1-2\mu)}{r^3(1-\mu)}\frac{\partial^2 u_r}{\partial\theta^2}-\frac{(1-2\mu)}{2r^2(1-\mu)}\frac{\partial^3 u_r}{\partial r\partial\theta^2}+\frac{2}{r^2}\frac{\partial u_r}{\partial r}-\frac{1}{r}\frac{\partial^2 u_r}{\partial r^2}-\frac{(3-4\mu)}{r^3(1-\mu)}\frac{\partial u_\theta}{\partial\theta}-\frac{2}{r^3}u_r, \tag{4a}$$

$$\frac{\partial^3 u_\theta}{\partial\theta^3}=-\frac{r^2(1-2\mu)}{2(1-\mu)}\frac{\partial^3 u_\theta}{\partial r^2\partial\theta}-\frac{r}{2(1-\mu)}\frac{\partial^3 u_r}{\partial r\partial\theta^2}-\frac{r(1-2\mu)}{2(1-\mu)}\frac{\partial^2 u_\theta}{\partial r\partial\theta}-\frac{(3-4\mu)}{2(1-\mu)}\frac{\partial^2 u_r}{\partial\theta^2}+\frac{(1-2\mu)}{2(1-\mu)}\frac{\partial u_\theta}{\partial\theta}. \tag{4b}$$

Equations (4a) and (4b) are substituted into Eq. (3c), the final result is simplified as follows:

$$\frac{1}{r}\frac{\partial^2 u_r}{\partial r^2}+\frac{1}{2r^2(1-\mu)}\frac{\partial^2 u_\theta}{\partial r\partial\theta}+\frac{(1-2\mu)}{2r^3(1-\mu)}\frac{\partial^2 u_r}{\partial\theta^2}+\frac{1}{r^2}\frac{\partial u_r}{\partial r}-\frac{(3-4\mu)}{2r^3(1-\mu)}\frac{\partial u_\theta}{\partial\theta}-\frac{u_r}{r^3}=0. \tag{4c}$$

Comparing Eqs. (3a) and (4c), it can be seen that the two equations have the same solution. Thus, Eq. (3c) is redundant for Eqs. (3a) and (3b). Therefore, Eqs. (3a) and (3b) are the governing equations for solving the plane elasticity problem with displacement components in polar coordinates. The solution satisfying both Eqs. (3a), (3b) and boundary conditions should be the exact solution. However, Eqs. (3a) and (3b) are elliptic partial differential equations with variable coefficients. At the same time, boundary conditions are often mixed modes of stress and displacement boundary conditions. Therefore, the exact solution to this problem is not always an easy task theoretically. An alternative mathematical method is transforming the terms of two variables in partial differential equations into a single variable with all possible modes of boundary conditions.

3 Governing equations expressed by displacement function

In order reduce the two variables $u_r(r,\theta)$ and $u_\theta(r,\theta)$ in the control equation to a single variable, a new displacement function $\psi(r,\theta)$ is introduced in the present paper; it is defined as follows:

$$u_r=\alpha_1\frac{\partial^2\psi}{\partial r^2}+\alpha_2\frac{1}{r}\frac{\partial^2\psi}{\partial r\partial\theta}+\alpha_3\frac{1}{r^2}\frac{\partial^2\psi}{\partial\theta^2}+\alpha_4\frac{1}{r}\frac{\partial\psi}{\partial r}+\alpha_5\frac{1}{r^2}\frac{\partial\psi}{\partial\theta}+\alpha_6\frac{1}{r^2}\psi, \tag{5a}$$

$$u_\theta=\alpha_7\frac{\partial^2\psi}{\partial r^2}+\alpha_8\frac{1}{r}\frac{\partial^2\psi}{\partial r\partial\theta}+\alpha_9\frac{1}{r^2}\frac{\partial^2\psi}{\partial\theta^2}+\alpha_{10}\frac{1}{r}\frac{\partial\psi}{\partial r}+\alpha_{11}\frac{1}{r^2}\frac{\partial\psi}{\partial\theta}+\alpha_{12}\frac{1}{r^2}\psi, \tag{5b}$$

where the coefficient α_i $(i=1,2,3,\ldots,12)$ is the material constants [27].

Substituting Eqs. (5a) and (5b) into Eqs. (3a) and (3b), the governing equations expressed by the displacement function are given as follows:

$$
\begin{aligned}
&\alpha_1\frac{\partial^4\psi}{\partial r^4}+\frac{1}{r}\left\{\alpha_2+\frac{1}{2(1-\mu)}\alpha_7\right\}\frac{\partial^4\psi}{\partial r^3\partial\theta}\\
&\quad+\frac{1}{r^2}\left\{\frac{1-2\mu}{2(1-\mu)}\alpha_1+\alpha_3+\frac{1}{2(1-\mu)}\alpha_8\right\}\frac{\partial^4\psi}{\partial r^2\partial\theta^2}\\
&\quad+\frac{1}{r^3}\left\{\frac{1-2\mu}{2(1-\mu)}\alpha_2+\frac{1}{2(1-\mu)}\alpha_9\right\}\frac{\partial^4\psi}{\partial r\partial\theta^3}+\frac{1}{r^4}\left\{\frac{1-2\mu}{2(1-\mu)}\alpha_3\right\}\frac{\partial^4\psi}{\partial\theta^4}\\
&\quad+\frac{1}{r}\{\alpha_1+\alpha_4\}\frac{\partial^3\psi}{\partial r^3}+\frac{1}{r^2}\left\{-\alpha_2+\alpha_5-\frac{3-4\mu}{2(1-\mu)}\alpha_7+\frac{1}{2(1-\mu)}\alpha_{10}\right\}\frac{\partial^3\psi}{\partial r^2\partial\theta}\\
&\quad+\frac{1}{r^3}\left\{-3\alpha_3+\frac{1-2\mu}{2(1-\mu)}\alpha_4-2\alpha_8+\frac{1}{2(1-\mu)}\alpha_{11}\right\}\frac{\partial^3\psi}{\partial r\partial\theta^2}\\
&\quad+\frac{1}{r^4}\left\{\frac{1-2\mu}{2(1-\mu)}\alpha_5+\frac{-5+4\mu}{2(1-\mu)}\alpha_9\right\}\frac{\partial^3\psi}{\partial\theta^3}+\frac{1}{r^2}\{-\alpha_1-\alpha_4+\alpha_6\}\frac{\partial^2\psi}{\partial r^2}\\
&\quad+\frac{1}{r^3}\left\{-3\alpha_5-2\alpha_{10}+\frac{1}{2(1-\mu)}\alpha_{12}\right\}\frac{\partial^2\psi}{\partial r\partial\theta}\\
&\quad+\frac{1}{r^4}\left\{3\alpha_3+\frac{1-2\mu}{2(1-\mu)}\alpha_6-\frac{5-4\mu}{2(1-\mu)}\alpha_{11}\right\}\frac{\partial^2\psi}{\partial\theta^2}\\
&\quad+\frac{1}{r^3}\{-3\alpha_6\}\frac{\partial\psi}{\partial r}+\frac{1}{r^4}\left\{3\alpha_5-\frac{5-4\mu}{2(1-\mu)}\alpha_{12}\right\}\frac{\partial\psi}{\partial\theta}+\frac{1}{r^4}\{3\alpha_6\}\psi=0,
\end{aligned}
\tag{6a}
$$

$$
\begin{aligned}
&\frac{1-2\mu}{2(1-\mu)}\alpha_7\frac{\partial^4\psi}{\partial r^4}+\frac{1}{r}\left\{\frac{1}{2(1-\mu)}\alpha_1+\frac{1-2\mu}{2(1-\mu)}\alpha_8\right\}\frac{\partial^4\psi}{\partial r^3\partial\theta}\\
&\quad+\frac{1}{r^2}\left\{\frac{1}{2(1-\mu)}\alpha_2+\alpha_7+\frac{1-2\mu}{2(1-\mu)}\alpha_9\right\}\frac{\partial^4\psi}{\partial r^2\partial\theta^2}\\
&\quad+\frac{1}{r^3}\left\{\frac{1}{2(1-\mu)}\alpha_3+\alpha_8\right\}\frac{\partial^4\psi}{\partial r\partial\theta^3}\\
&\quad+\frac{1}{r^4}\{\alpha_9\}\frac{\partial^4\psi}{\partial\theta^4}+\frac{1}{r}\left\{\frac{1-2\mu}{2(1-\mu)}\alpha_7+\frac{1-2\mu}{2(1-\mu)}\alpha_{10}\right\}\frac{\partial^3\psi}{\partial r^3}\\
&\quad+\frac{1}{r^2}\left\{\frac{3-4\mu}{2(1-\mu)}\alpha_1+\frac{1}{2(1-\mu)}\alpha_4-\frac{1-2\mu}{2(1-\mu)}\alpha_8+\frac{1-2\mu}{2(1-\mu)}\alpha_{11}\right\}\frac{\partial^3\psi}{\partial r^2\partial\theta}\\
&\quad+\frac{1}{r^3}\left\{\frac{1-2\mu}{1-\mu}\alpha_2+\frac{1}{2(1-\mu)}\alpha_5-\frac{3(1-2\mu)}{2(1-\mu)}\alpha_9+\alpha_{10}\right\}\frac{\partial^3\psi}{\partial r\partial\theta^2}\\
&\quad+\frac{1}{r^4}\left\{\frac{1-4\mu}{2(1-\mu)}\alpha_3+\alpha_{11}\right\}\frac{\partial^3\psi}{\partial\theta^3}\\
&\quad+\frac{1}{r^2}\left\{-\frac{1-2\mu}{2(1-\mu)}\alpha_7-\frac{1-2\mu}{2(1-\mu)}\alpha_{10}+\frac{1-2\mu}{2(1-\mu)}\alpha_{12}\right\}\frac{\partial^2\psi}{\partial r^2}\\
&\quad+\frac{1}{r^3}\left\{\frac{1-2\mu}{1-\mu}\alpha_4+\frac{1}{2(1-\mu)}\alpha_6-\frac{3(1-2\mu)}{2(1-\mu)}\alpha_{11}\right\}\frac{\partial^2\psi}{\partial r\partial\theta}\\
&\quad+\frac{1}{r^4}\left\{\frac{1-4\mu}{2(1-\mu)}\alpha_5+\frac{3(1-2\mu)}{2(1-\mu)}\alpha_9+\alpha_{12}\right\}\frac{\partial^2\psi}{\partial\theta^2}+\frac{1}{r^3}\left\{-\frac{3(1-2\mu)}{2(1-\mu)}\alpha_{12}\right\}\frac{\partial\psi}{\partial r}\\
&\quad+\frac{1}{r^4}\left\{\frac{1-4\mu}{2(1-\mu)}\alpha_6+\frac{3(1-2\mu)}{2(1-\mu)}\alpha_{11}\right\}\frac{\partial\psi}{\partial\theta}+\frac{1}{r^4}\left\{\frac{3(1-2\mu)}{2(1-\mu)}\alpha_{12}\right\}\psi=0.
\end{aligned}
\tag{6b}
$$

Here, for solving the variable $\psi(r,\theta)$ with two governing equations, it is necessary to determine some coefficients α_i $(i = 1, 2, 3, \ldots, 12)$ reasonably that make one of the two governing equations redundant. Mathematically, it is required that one equation of Eqs. (6a)–(6b) can be satisfied under all circumstances. However, it is obvious that all the partial derivatives of the displacement function $\psi(r,\theta)$ as well as itself cannot be vanished only when the coefficients of all the derivatives of $\psi(r,\theta)$ as well as itself are zero.

3.1 Governing equation—Form I

It is assumed that Eq. (6a) is satisfied automatically, and Eq. (6b) is the governing equation in terms of the displacement function $\psi(r,\theta)$. Let the coefficients of $\psi(r,\theta)$ as well as all its derivatives in Eq. (6a) equate to zero, the coefficients α_i $(i = 1, 2, 3, \ldots, 12)$ are obtained as follows:

$$\alpha_i = 0 \quad (i = 1, 3, 4, 6, 8, 11), \tag{7a}$$

$$\alpha_2 = -\frac{1}{2(1-\mu)}, \tag{7b}$$

$$\alpha_5 = \frac{(5-4\mu)}{2(1-\mu)}, \tag{7c}$$

$$\alpha_7 = 1, \tag{7d}$$

$$\alpha_9 = \frac{(1-2\mu)}{2(1-\mu)}, \tag{7e}$$

$$\alpha_{10} = -3, \tag{7f}$$

$$\alpha_{12} = 3. \tag{7g}$$

And the governing equation in terms of the displacement function $\psi(r,\theta)$ is

$$\begin{aligned}&\frac{\partial^4\psi}{\partial r^4} + \frac{1}{r^4}\frac{\partial^4\psi}{\partial\theta^4} + \frac{2}{r^2}\frac{\partial^4\psi}{\partial r^2\partial\theta^2} - \frac{2}{r}\frac{\partial^3\psi}{\partial r^3} - \frac{6}{r^3}\frac{\partial^3\psi}{\partial r\partial\theta^2} + \frac{5}{r^2}\frac{\partial^2\psi}{\partial r^2} + \frac{10}{r^4}\frac{\partial^2\psi}{\partial\theta^2}\\ &\quad - \frac{9}{r^3}\frac{\partial\psi}{\partial r} + \frac{9}{r^4}\psi = 0.\end{aligned} \tag{8}$$

Equation (8) gives the exact expression of the governing equation of the displacement function for the plane elastic problem in polar coordinates. It is not difficult to conclude that the displacement function governing equation is a partial differential equation that is independent of the material constants such as elastic modulus E and Poisson's ratio μ.

3.2 Governing equation—Form II

It is assumed that Eq. (6b) is satisfied automatically, and Eq. (6a) is the governing equation in terms of the displacement function $\psi(r,\theta)$. Let the coefficients of $\psi(r,\theta)$ as well as all its derivatives in Eq. (6b) equate to zero, the coefficients α_i $(i = 1, 2, 3, \ldots, 12)$ are obtained as follows:

$$\alpha_i = 0 \quad (i = 2, 5, 7, 9, 10, 12), \tag{9a}$$

$$\alpha_1 = -\frac{(1-2\mu)}{(1-4\mu)}, \tag{9b}$$

$$\alpha_3 = -\frac{2(1-\mu)}{(1-4\mu)}, \tag{9c}$$

$$\alpha_4 = \frac{3(1-2\mu)}{(1-4\mu)}, \tag{9d}$$

$$\alpha_6 = -\frac{3(1-2\mu)}{(1-4\mu)}, \tag{9e}$$

$$\alpha_8 = \frac{1}{(1-4\mu)}, \tag{9f}$$

$$\alpha_{11} = 1. \tag{9g}$$

And the control equation in terms of the displacement function $\psi(r,\theta)$ is

$$\begin{aligned}&\frac{\partial^4\psi}{\partial r^4} + \frac{1}{r^4}\frac{\partial^4\psi}{\partial\theta^4} + \frac{2}{r^2}\frac{\partial^4\psi}{\partial r^2\partial\theta^2} - \frac{2}{r}\frac{\partial^3\psi}{\partial r^3} - \frac{6}{r^3}\frac{\partial^3\psi}{\partial r\partial\theta^2} + \frac{5}{r^2}\frac{\partial^2\psi}{\partial r^2} + \frac{10}{r^4}\frac{\partial^2\psi}{\partial\theta^2}\\ &\quad - \frac{9}{r^3}\frac{\partial\psi}{\partial r} + \frac{9}{r^4}\psi = 0.\end{aligned} \tag{10}$$

It is obvious that the partial differential equations in terms of displacement function given by Eq. (8) and (10) are identical, that is, the displacement function governing equations I and II are the same equation. That is, the governing equation expressed by the displacement function $\psi(r,\theta)$ is unique.

4 Displacement components and stress components expressed by displacement function

To solve the displacement function governing Eqs. (8) or (10), it is necessary to know the displacement boundary conditions or stress boundary conditions at each point on the boundary. However, the displacement boundary conditions of the elastic body are often known displacements, and the stress boundary conditions are often known loadings. Therefore, it is necessary to express the known displacement components and stress components as the partial derivative in terms of the displacement function $\psi(r,\theta)$.

The displacement components of the plane strain problem in polar coordinates are the radial displacement $u_r(r,\theta)$ and the circumferential displacement $u_\theta(r,\theta)$, and the stress components are the radial stress σ_r, the circumferential stress σ_θ, and the shear stress $\tau_{r\theta}$.

Equations (5a)–(5b) is substituted into Eqs. (2a)–(2c), the stress components are expressed by the displacement function as follows in the case of plane strain:

$$\begin{aligned}\sigma_r = {}& \frac{E(1-\mu)}{(1-2\mu)(1+\mu)}\\ &\times\left[\begin{array}{c}\alpha_1\frac{\partial^3\psi}{\partial r^3} + \frac{1}{r}(\alpha_2 + \frac{\mu}{1-\mu}\alpha_7)\frac{\partial^3\psi}{\partial r^2\partial\theta} + \frac{1}{r^2}(\alpha_3 + \frac{\mu}{1-\mu}\alpha_8)\frac{\partial^3\psi}{\partial r\partial\theta^2} + \frac{1}{r^3}(\frac{\mu}{1-\mu}\alpha_9)\frac{\partial^3\psi}{\partial\theta^3}\\ + \frac{1}{r}(\frac{\mu}{1-\mu}\alpha_1 + \alpha_4)\frac{\partial^2\psi}{\partial r^2} + \frac{1}{r^2}(-\frac{1-2\mu}{1-\mu}\alpha_2 + \alpha_5 + \frac{\mu}{1-\mu}\alpha_{10})\frac{\partial^2\psi}{\partial r\partial\theta}\\ + \frac{1}{r^3}(-\frac{2-3\mu}{1-\mu}\alpha_3 + \frac{\mu}{1-\mu}\alpha_{11})\frac{\partial^2\psi}{\partial\theta^2} + \frac{1}{r^2}(-\frac{1-2\mu}{1-\mu}\alpha_4 + \alpha_6)\frac{\partial\psi}{\partial r}\\ + \frac{1}{r^3}(-\frac{2-3\mu}{1-\mu}\alpha_5 + \frac{\mu}{1-\mu}\alpha_{12})\frac{\partial\psi}{\partial\theta} + \frac{1}{r^3}(-\frac{2-3\mu}{1-\mu}\alpha_6)\psi\end{array}\right],\end{aligned} \tag{11a}$$

$$\sigma_\theta = \frac{E(1-\mu)}{(1-2\mu)(1+\mu)} \times \begin{bmatrix} \frac{\mu}{1-\mu}\alpha_1\frac{\partial^3\psi}{\partial r^3} + \frac{1}{r}(\frac{\mu}{1-\mu}\alpha_2+\alpha_7)\frac{\partial^3\psi}{\partial r^2\partial\theta} + \frac{1}{r^2}(\frac{\mu}{1-\mu}\alpha_3+\alpha_8)\frac{\partial^3\psi}{\partial r\partial\theta^2} + \frac{1}{r^3}\alpha_9\frac{\partial^3\psi}{\partial\theta^3} \\ + \frac{1}{r}(\alpha_1+\frac{\mu}{1-\mu}\alpha_4)\frac{\partial^2\psi}{\partial r^2} + \frac{1}{r^2}(\frac{1-2\mu}{1-\mu}\alpha_2+\frac{\mu}{1-\mu}\alpha_5+\alpha_{10})\frac{\partial^2\psi}{\partial r\partial\theta} \\ + \frac{1}{r^3}(\frac{1-3\mu}{1-\mu}\alpha_3+\alpha_{11})\frac{\partial^2\psi}{\partial\theta^2} + \frac{1}{r^2}(\frac{1-2\mu}{1-\mu}\alpha_4+\frac{\mu}{1-\mu}\alpha_6)\frac{\partial\psi}{\partial r} \\ + \frac{1}{r^3}(\frac{1-3\mu}{1-\mu}\alpha_5+\alpha_{12})\frac{\partial\psi}{\partial\theta} + \frac{1}{r^3}\frac{1-3\mu}{1-\mu}\alpha_6\psi \end{bmatrix}, \tag{11b}$$

$$\tau_{r\theta} = \frac{E}{2(1+\mu)} \times \begin{bmatrix} \alpha_7\frac{\partial^3\psi}{\partial r^3} + \frac{1}{r}(\alpha_1+\alpha_8)\frac{\partial^3\psi}{\partial r^2\partial\theta} + \frac{1}{r^2}(\alpha_2+\alpha_9)\frac{\partial^3\psi}{\partial r\partial\theta^2} + \frac{1}{r^3}\alpha_3\frac{\partial^3\psi}{\partial\theta^3} \\ + \frac{1}{r}(-\alpha_7+\alpha_{10})\frac{\partial^2\psi}{\partial r^2} + \frac{1}{r^2}(\alpha_4-2\alpha_8+\alpha_{11})\frac{\partial^2\psi}{\partial r\partial\theta} + \frac{1}{r^3}(\alpha_5-3\alpha_9)\frac{\partial^2\psi}{\partial\theta^2} \\ + \frac{1}{r^2}(\alpha_{12}-2\alpha_{10})\frac{\partial\psi}{\partial r} + \frac{1}{r^3}(\alpha_6-3\alpha_{11})\frac{\partial\psi}{\partial\theta} + \frac{1}{r^3}(-3\alpha_{12})\psi \end{bmatrix}. \tag{11c}$$

4.1 Displacement and stress expressions—Form I

Substituting the values of α_i in Eqs. (7a)–(7g) into Eqs. (5a)–(5b), the displacement components expressions are as follows:

$$u_r(r,\theta) = -\frac{1}{2r(1-\mu)}\frac{\partial^2\psi}{\partial r\partial\theta} + \frac{(5-4\mu)}{2r^2(1-\mu)}\frac{\partial\psi}{\partial\theta}, \tag{12a}$$

$$u_\theta(r,\theta) = \frac{\partial^2\psi}{\partial r^2} + \frac{(1-2\mu)}{2r^2(1-\mu)}\frac{\partial^2\psi}{\partial\theta^2} - \frac{3}{r}\frac{\partial\psi}{\partial r} + \frac{3}{r^2}\psi. \tag{12b}$$

Substituting the values of α_i in Eqs. (7a)–(7g) into Eqs. (11a)–(11c), the stress components expressions are as follows:

$$\sigma_r = \frac{E}{2(1+\mu)}\left[-\frac{1}{r}\frac{\partial^3\psi}{\partial r^2\partial\theta} + \frac{\mu}{r^3(1-\mu)}\frac{\partial^3\psi}{\partial\theta^3} + \frac{(6-5\mu)}{r^2(1-\mu)}\frac{\partial^2\psi}{\partial r\partial\theta} - \frac{(10-9\mu)}{r^3(1-\mu)}\frac{\partial\psi}{\partial\theta}\right], \tag{13a}$$

$$\sigma_\theta = \frac{E}{2(1+\mu)}\left[\frac{(2-\mu)}{r(1-\mu)}\frac{\partial^3\psi}{\partial r^2\partial\theta} + \frac{1}{r^3}\frac{\partial^3\psi}{\partial\theta^3} - \frac{(7-5\mu)}{r^2(1-\mu)}\frac{\partial^2\psi}{\partial r\partial\theta} + \frac{(11-9\mu)}{r^3(1-\mu)}\frac{\partial\psi}{\partial\theta}\right], \tag{13b}$$

$$\tau_{r\theta} = \frac{E}{2(1+\mu)} \times \left[\frac{\partial^3\psi}{\partial r^3} - \frac{\mu}{r^2(1-\mu)}\frac{\partial^3\psi}{\partial r\partial\theta^2} - \frac{4}{r}\frac{\partial^2\psi}{\partial r^2} + \frac{1+\mu}{r^3(1-\mu)}\frac{\partial^2\psi}{\partial\theta^2} + \frac{9}{r^2}\frac{\partial\psi}{\partial r} - \frac{9}{r^3}\psi\right]. \tag{13c}$$

4.2 Displacement and stress expressions—Form II

Substituting the values of α_i in Eqs. (9a)–(9g) into Eqs. (5a)–(5b), the displacement components expressions are as follows:

$$u_r = \frac{(1-\mu)}{(1-4\mu)}\left[-\frac{(1-2\mu)}{(1-\mu)}\frac{\partial^2\psi}{\partial r^2} - \frac{2}{r^2}\frac{\partial^2\psi}{\partial\theta^2} + \frac{3(1-2\mu)}{r(1-\mu)}\frac{\partial\psi}{\partial r} - \frac{3(1-2\mu)}{r^2(1-\mu)}\psi\right], \tag{14a}$$

$$u_\theta = \frac{(1-\mu)}{(1-4\mu)}\left[\frac{1}{r(1-\mu)}\frac{\partial^2\psi}{\partial r\partial\theta} + \frac{(1-4\mu)}{r^2(1-\mu)}\frac{\partial\psi}{\partial\theta}\right]. \tag{14b}$$

Substituting the values of α_i in Eqs. (9a)–(9g) into Eqs. (11a)–(11c), the stress components expressions are as follows:

$$\sigma_r = \frac{E(1-\mu)}{(1+\mu)(1-4\mu)}\begin{bmatrix} -\frac{\partial^3\psi}{\partial r^3} - \frac{(2-\mu)}{r^2(1-\mu)}\frac{\partial^3\psi}{\partial r\partial\theta^2} + \frac{(3-4\mu)}{r(1-\mu)}\frac{\partial^2\psi}{\partial r^2} \\ + \frac{(4-\mu)}{r^3(1-\mu)}\frac{\partial^2\psi}{\partial\theta^2} - \frac{3(2-3\mu)}{r^2(1-\mu)}\frac{\partial\psi}{\partial r} + \frac{3(2-3\mu)}{r^3(1-\mu)}\psi \end{bmatrix}, \tag{15a}$$

$$\sigma_\theta = \frac{E(1-\mu)}{(1+\mu)(1-4\mu)} \begin{bmatrix} -\frac{\mu}{1-\mu}\frac{\partial^3\psi}{\partial r^3} + \frac{1}{r^2}\frac{\partial^3\psi}{\partial r\partial\theta^2} - \frac{(1-4\mu)}{r(1-\mu)}\frac{\partial^2\psi}{\partial r^2} \\ -\frac{1}{r^3}\frac{\partial^2\psi}{\partial\theta^2} + \frac{3(1-3\mu)}{r^2(1-\mu)}\frac{\partial\psi}{\partial r} - \frac{3(1-3\mu)}{r^3(1-\mu)}\psi \end{bmatrix}, \tag{15b}$$

$$\tau_{r\theta} = \frac{E(1-\mu)}{(1+\mu)(1-4\mu)} \times \left[\frac{\mu}{r(1-\mu)}\frac{\partial^3\psi}{\partial r^2\partial\theta} - \frac{1}{r^3}\frac{\partial^3\psi}{\partial\theta^3} + \frac{1-5\mu}{r^2(1-\mu)}\frac{\partial^2\psi}{\partial r\partial\theta} - \frac{3(1-3\mu)}{r^3(1-\mu)}\frac{\partial\psi}{\partial\theta}\right]. \tag{15c}$$

5 Finite difference scheme

In this section, the finite difference method is used to obtain the numerical solution of nodal values of the displacement function satisfying the governing equation. It is obvious that the governing equation in terms of the displacement function is a fourth-order elliptical partial differential equation with variable coefficients. At the same time, the stress expression expressed in terms of the displacement function is a third-order partial differential equation, and the displacement expression expressed in terms of the displacement function is a second-order partial differential equation.

All of these partial differential equations are transformed into their corresponding algebraic equations by using the finite difference method. The numerical calculation process is divided into three steps: Firstly, the values of the displacement function at each point of the domain are solved by the algebraic equations of the governing equations and the boundary conditions. Secondly, the partial derivative values of the displacement functions at each point are obtained by their difference equations. Finally, the displacement components and the stress components at each point are solved by the partial derivative values of the displacement function and the values of the displacement function.

5.1 Difference scheme of governing equation

The governing equation in terms of displacement function is suitable for solving the internal mesh points of the domain. According to Eq. (8), the governing equation is composed of total eight different partial derivatives of the displacement function of order ranging from one to four together with the displacement function itself. All the individual derivatives of the governing equation are replaced by their corresponding central difference expressions having local truncation errors of $o(h^2)$ and $o(k^2)$. The mesh length in r-direction (i-direction) is recorded as h, and the mesh length in θ-direction (j-direction) is recorded as k.

$$\left(\frac{\partial^4\psi}{\partial r^4}\right)_{i,j} = \frac{1}{h^4}[\psi_{i+2,j} - 4\psi_{i+1,j} + 6\psi_{i,j} - 4\psi_{i-1,j} + \psi_{i-2,j}], \tag{16a}$$

$$\left(\frac{\partial^4\psi}{\partial\theta^4}\right)_{i,j} = \frac{1}{k^4}[\psi_{i,j+2} - 4\psi_{i,j+1} + 6\psi_{i,j} - 4\psi_{i,j-1} + \psi_{i,j-2}], \tag{16b}$$

$$\left(\frac{\partial^4\psi}{\partial r^2\partial\theta^2}\right)_{i,j} = \frac{1}{h^2k^2}\begin{bmatrix} \psi_{i+1,j+1} - 2\psi_{i+1,j} + \psi_{i+1,j-1} - 2\psi_{i,j+1} + 4\psi_{i,j} \\ -2\psi_{i,j-1} + \psi_{i-1,j+1} - 2\psi_{i-1,j} + \psi_{i-1,j-1} \end{bmatrix}, \tag{16c}$$

$$\left(\frac{\partial^3\psi}{\partial r^3}\right)_{i,j} = \frac{1}{2h^3}[\psi_{i+2,j} - 2\psi_{i+1,j} + 2\psi_{i-1,j} - \psi_{i-2,j}], \tag{16d}$$

$$\left(\frac{\partial^3\psi}{\partial r\partial\theta^2}\right)_{i,j} = \frac{1}{2hk^2}[\psi_{i+1,j+1} - 2\psi_{i+1,j} + \psi_{i+1,j-1} - \psi_{i-1,j+1} + 2\psi_{i-1,j} - \psi_{i-1,j-1}], \tag{16e}$$

$$\left(\frac{\partial^2\psi}{\partial r^2}\right)_{i,j} = \frac{1}{h^2}[\psi_{i+1,j} - 2\psi_{i,j} + \psi_{i-1,j}], \tag{16f}$$

$$\left(\frac{\partial^2\psi}{\partial \theta^2}\right)_{i,j} = \frac{1}{k^2}[\psi_{i,j+1} - 2\psi_{i,j} + \psi_{i,j-1}], \tag{16g}$$

$$\left(\frac{\partial\psi}{\partial r}\right)_{i,j} = \frac{1}{2h}[\psi_{i+1,j} - \psi_{i-1,j}]. \tag{16h}$$

Substituting Eqs. (16a)–(16h) into Eq. (8), the governing equation for solving the internal mesh points of the domain is written in terms of nodal unknowns of the displacement function ψ as follows:

$$\begin{aligned}&\xi_1\psi(i+2,j) + \xi_2\psi(i+1,j+1) + \xi_3\psi(i+1,j) + \xi_2\psi(i+1,j-1) + \xi_4\psi(i,j+2)\\ &\quad + \xi_5\psi(i,j+1) + \xi_6\psi(i,j) + \xi_5\psi(i,j-1) + \xi_4\psi(i,j-2) + \xi_7\psi(i-1,j+1)\\ &\quad + \xi_8\psi(i-1,j) + \xi_7\psi(i-1,j-1) + \xi_9\psi(i-2,j) = 0,\end{aligned} \tag{17}$$

where

$$\begin{aligned}\xi_1 &= r_i^3k^4(r_i - h),\\ \xi_2 &= r_ih^2k^2(2r_i - 3h),\\ \xi_3 &= r_ik^2\left[-4r_i^3k^2 - 4r_ih^2 + 2r_i^2hk^2 + 6h^3 + 5r_ih^2k^2 - 4.5h^3k^2\right],\\ \xi_4 &= h^4,\\ \xi_5 &= 2h^2\left(-2h^2 - 2r_i^2k^2 + 5h^2k^2\right),\\ \xi_6 &= 6r_i^4k^4 + 6h^4 + 8r_i^2h^2k^2 - 10r_i^2h^2k^2 - 20h^4k^2 + 9h^4k^4,\\ \xi_7 &= r_ih^2k^2(2r_i + 3h),\\ \xi_8 &= r_ik^2\left(-4r_i^3k^2 - 4r_ih^2 - 2r_i^2hk^2 - 6h^3 + 5r_ih^2k^2 + 4.5h^3k^2\right),\\ \xi_9 &= r_i^3k^4(r_i + h).\end{aligned}$$

The finite difference scheme of the governing equation at one node is symmetric about both r- and θ-axes, and the computational domain at one node involves thirteen neighboring nodes. Obviously, when the node (i,j) is close to the real boundary, the computational domain does not only involve the real boundary, but also involves a layer of imaginary nodes. The boundary formed by a layer of imaginary nodes is called an imaginary layer which is outside the real boundary.

5.2 Difference scheme of displacement components

It can be seen that the radial displacement component and the hoop displacement component are the second-order partial derivatives of the displacement function. Unlike the case of governing equations, the central difference method has been avoided for the displacement components because most of time they are found to include nodes exterior to the imaginary layer. Therefore, on the basis of keeping the order of local truncation error also to be $o(h^2)$ or $o(k^2)$, different finite differencing schemes (for example, forward difference, backward difference, and center difference) are adopted for different derivatives present

in the displacement components. It should be noted that the expression of the displacement component has two Forms (Form-I and Form-II), and in the following section, only the difference formula of the displacement components in Form-I is given. The difference formula of displacement components in Form-II is similar to that in Form-I.

For radial displacement, four different versions of finite difference formulas have been developed for points on different regions of the boundary. These versions of finite difference formulas are obtained by adapting different combinations of forward and backward differencing schemes in both r- and θ- directions. Here, the differential formulas of four radial displacements are given. It is observed that the radial displacement component contains nine nodes in the computational domain, but no nodes beyond the imaginary layer.

(a) r-forward difference, θ-forward difference:

$$\begin{aligned} u_r(i,j) &= a_1\psi(i+2,j+2) - 4a_1\psi(i+2,j+1) + 3a_1\psi(i+2,j) \\ &\quad - 4a_1\psi(i+1,j+2) + 16a_1\psi(i+1,j+1) - 12a_1\psi(i+1,j) \\ &\quad + (3a_1 - b_1)\psi(i,j+2) - (12a_1 - 4b_1)\psi(i,j+1) \\ &\quad + (9a_1 - 3b_1)\psi(i,j), \end{aligned} \tag{18}$$

where $a_1 = -\frac{1}{8r_i hk(1-\mu)}$, $b_1 = \frac{5-4\mu}{4r_i^2 k(1-\mu)}$;

(b) r-forward difference, θ-backward difference:

$$\begin{aligned} u_r(i,j) &= -3a_1\psi(i+2,j) + 4a_1\psi(i+2,j-1) - a_1\psi(i+2,j-2) \\ &\quad + 12a_1\psi(i+1,j) - 16a_1\psi(i+1,j-1) + 4a_1\psi(i+1,j-2) \\ &\quad - (9a_1 - 3b_1)\psi(i,j) + (12a_1 - 4b_1)\psi(i,j-1) \\ &\quad - (3a_1 - b_1)\psi(i,j-2), \end{aligned} \tag{19}$$

where $a_1 = -\frac{1}{8r_i hk(1-\mu)}$, $b_1 = \frac{5-4\mu}{4r_i^2 k(1-\mu)}$;

(c) r-backward difference, θ-forward difference:

$$\begin{aligned} u_r(i,j) &= -(3a_1 + b_1)\psi(i,j+2) + (12a_1 + 4b_1)\psi(i,j+1) - (9a_1 + 3b_1)\psi(i,j) \\ &\quad + 4a_1\psi(i-1,j+2) - 16a_1\psi(i-1,j+1) + 12a_1\psi(i-1,j) \\ &\quad - a_1\psi(i-2,j+2) + 4a_1\psi(i-2,j+1) - 3a_1\psi(i-2,j), \end{aligned} \tag{20}$$

where $a_1 = -\frac{1}{8r_i hk(1-\mu)}$, $b_1 = \frac{5-4\mu}{4r_i^2 k(1-\mu)}$;

(d) r-backward difference, θ-backward difference:

$$\begin{aligned} u_r(i,j) &= (9a_1 + 3b_1)\psi(i,j) - (12a_1 + 4b_1)\psi(i,j-1) + (3a_1 + b_1)\psi(i,j-2) \\ &\quad - 12a_1\psi(i-1,j) + 16a_1\psi(i-1,j-1) - 4a_1\psi(i-1,j-2) \\ &\quad + 3a_1\psi(i-2,j) - 4a_1\psi(i-2,j-1) + a_1\psi(i-2,j-2), \end{aligned} \tag{21}$$

where $a_1 = -\frac{1}{8r_i hk(1-\mu)}$, $b_1 = \frac{5-4\mu}{4r_i^2 k(1-\mu)}$.

For the hoop displacement component in the computational domain, only five nodes are involved, and the five node positions are symmetric about both r- and θ-directions. Therefore, only one difference formula is given for the hoop displacement component in the computational domain. It can be applied for points on any region of the boundary without the inclusion of nodes exterior to the imaginary layer.

$$\begin{aligned} u_\theta(i,j) &= (a_2 + c_2)\psi(i+1,j) + b_2\psi(i,j+1) + (-2a_2 - 2b_2 + d_2)\psi(i,j) \\ &\quad + b_2\psi(i,j-1) + (a_2 - c_2)\psi(i-1,j), \end{aligned} \tag{22}$$

where $a_2 = \frac{1}{h^2}$, $b_2 = \frac{1-2\mu}{2r_i^2k^2(1-\mu)}$, $c_2 = -\frac{3}{2r_ih}$, $d_2 = \frac{3}{r_i^2}$.

5.3 Difference scheme of stress components

For the stress components, only the difference formula of the stress components in Form I is given. Here, two different finite difference formulas have been developed using the various combinations of central difference, forward difference, and back difference schemes for the individual derivatives. It should be mentioned that the difference schemes for stress components are divided into four situations: r center difference–θ forward difference, r center difference–θ backward difference, r forward difference–θ center difference, and r backward difference–θ center difference. In order to ensure that the nodes involved in the computational domain do not exceed the imaginary layer, the combination of different difference schemes is also adopted for some partial derivatives.

For example, in the difference scheme of r center difference–θ forward difference, although the forward difference in θ-direction is specified, the combination of center difference for a second-order derivative of the displacement function $\psi(r,\theta)$ and the forward difference for a first-order derivative of the displacement function $\psi(r,\theta)$ is used for the difference scheme for a third-order derivative of the displacement function $\psi(r,\theta)$. This can ensure that the number of difference algebraic equations is equal to the number of nodes in the computational domain.

(1) Difference equations of radial stress component σ_r and circumferential stress component σ_θ.

(a) r-center difference, θ-forward difference:

$$\begin{aligned} \sigma_r(i,j) &= (-A_1 - C_1)\psi(i+1,j+2) + (4A_1 + 4C_1)\psi(i+1,j+1) \\ &\quad + (-3A_1 - 3C_1)\psi(i+1,j) - B_1\psi(i,j+3) + (2A_1 + 6B_1)\psi(i,j+2) \\ &\quad + (-8A_1 - 12B_1 + D_1)\psi(i,j+1) + (6A_1 + 10B_1)\psi(i,j) \\ &\quad + (-3B_1 - D_1)\psi(i,j-1) + (-A_1 + C_1)\psi(i-1,j+2) \\ &\quad + (4A_1 - 4C_1)\psi(i-1,j+1) + (-3A_1 + 3C_1)\psi(i-1,j), \end{aligned} \tag{23}$$

where $A_1 = -\frac{E}{4r_ih^2k(1+\mu)}$, $B_1 = \frac{\mu E}{4r_i^3k^3(1-\mu^2)}$, $C_1 = \frac{E(6-5\mu)}{8r_i^2hk(1-\mu^2)}$, $D_1 = -\frac{E(10-9\mu)}{4r_i^3k(1-\mu^2)}$,

$$\begin{aligned} \sigma_\theta(i,j) &= (-A_2 - C_2)\psi(i+1,j+2) + (4A_2 + 4C_2)\psi(i+1,j+1) \\ &\quad + (-3A_2 - 3C_2)\psi(i+1,j) - B_2\psi(i,j+3) + (2A_2 + 6B_2)\psi(i,j+2) \\ &\quad + (-8A_2 - 12B_2 + D_2)\psi(i,j+1) + (6A_2 + 10B_2)\psi(i,j) \end{aligned}$$

$$
\begin{aligned}
&+(-3B_2-D_2)\psi(i,j-1)+(-A_2+C_2)\psi(i-1,j+2)\\
&+(4A_2-4C_2)\psi(i-1,j+1)+(-3A_2+3C_2)\psi(i-1,j),
\end{aligned}
\tag{24}
$$

where $A_2=\frac{E(2-\mu)}{4r_ih^2k(1-\mu^2)}$, $B_2=\frac{E}{4r_i^3k^3(1+\mu)}$, $C_2=-\frac{E(7-5\mu)}{8r_i^2hk(1-\mu^2)}$, $D_2=\frac{E(11-9\mu)}{4r_i^3k(1-\mu^2)}$;

(b) r-center difference, θ-backward difference:

$$
\begin{aligned}
\sigma_r(i,j)&=(3A_1+3C_1)\psi(i+1,j)+(-4A_1-4C_1)\psi(i+1,j-1)\\
&+(A_1+C_1)\psi(i+1,j-2)+(3B_1+D_1)\psi(i,j+1)\\
&+(-6A_1-10B_1)\psi(i,j)+(8A_1+12B_1-D_1)\psi(i,j-1)\\
&+(-2A_1-6B_1)\psi(i,j-2)+B_1\psi(i,j-3)+(3A_1-3C_1)\psi(i-1,j)\\
&+(-4A_1+4C_1)\psi(i-1,j-1)+(A_1-C_1)\psi(i-1,j-2),
\end{aligned}
\tag{25}
$$

where $A_1=-\frac{E}{4r_ih^2k(1+\mu)}$, $B_1=\frac{\mu E}{4r_i^3k^3(1-\mu^2)}$, $C_1=\frac{E(6-5\mu)}{8r_i^2hk(1-\mu^2)}$, $D_1=-\frac{E(10-9\mu)}{4r_i^3k(1-\mu^2)}$,

$$
\begin{aligned}
\sigma_\theta(i,j)&=(3A_2+3C_2)\psi(i+1,j)+(-4A_2-4C_2)\psi(i+1,j-1)\\
&+(A_2+C_2)\psi(i+1,j-2)+(3B_2+D_2)\psi(i,j+1)\\
&+(-6A_2-10B_2)\psi(i,j)+(8A_2+12B_2-D_2)\psi(i,j-1)\\
&+(-2A_2-6B_2)\psi(i,j-2)+B_2\psi(i,j-3)+(3A_2-3C_2)\psi(i-1,j)\\
&+(-4A_2+4C_2)\psi(i-1,j-1)+(A_2-C_2)\psi(i-1,j-2),
\end{aligned}
\tag{26}
$$

where $A_2=\frac{E(2-\mu)}{4r_ih^2k(1-\mu^2)}$, $B_2=\frac{E}{4r_i^3k^3(1+\mu)}$, $C_2=-\frac{E(7-5\mu)}{8r_i^2hk(1-\mu^2)}$, $D_2=\frac{E(11-9\mu)}{4r_i^3k(1-\mu^2)}$;

(2) Difference equation of shear stress $\tau_{r\theta}$

(a) r-forward difference, θ-center difference:

$$
\begin{aligned}
\tau_{r\theta}(i,j)&=-A_3\psi(i+3,j)-B_3\psi(i+2,j+1)+(6A_3+2B_3)\psi(i+2,j)\\
&-B_3\psi(i+2,j-1)+4B_3\psi(i+1,j+1)\\
&+(-12A_3-8B_3+C_3+E_3)\psi(i+1,j)+4B_3\psi(i+1,j-1)\\
&+(-3B_3+D_3)\psi(i,j+1)+(10A_3+6B_3-2C_3-2D_3+F_3)\psi(i,j)\\
&+(-3B_3+D_3)\psi(i,j-1)+(-3A_3+C_3-E_3)\psi(i-1,j),
\end{aligned}
\tag{27}
$$

where $A_3=\frac{E}{4r^3(1+\mu)}$, $B_3=-\frac{\mu E}{4r_i^2hk^2(1-\mu^2)}$, $C_3=-\frac{2E}{r_ih^2(1+\mu)}$, $D_3=\frac{E}{2r_i^3k^2(1-\mu)}$,
$E_3=\frac{9E}{4r_i^2h(1+\mu)}$, $F_3=-\frac{9E}{2r_i^3(1+\mu)}$;

(b) r-backward difference, θ-center difference:

$$
\begin{aligned}
\tau_{r\theta}(i,j)&=(3A_3+C_3+E_3)\psi(i+1,j)+(3B_3+D_3)\psi(i,j+1)\\
&+(-10A_3-6B_3-2C_3-2D_3+F_3)\psi(i,j)+(3B_3+D_3)\psi(i,j-1)\\
&-4B_3\psi(i-1,j+1)+(12A_3+8B_3+C_3-E_3)\psi(i-1,j)\\
&-4B_3\psi(i-1,j-1)+B_3\psi(i-2,j+1)-(6A_3+2B_3)\psi(i-2,j)\\
&+B_3\psi(i-2,j-1)+A_3\psi(i-3,j),
\end{aligned}
\tag{28}
$$

where $A_3 = \frac{E}{4r^3(1+\mu)}$, $B_3 = -\frac{\mu E}{4r_i^2 hk^2(1-\mu^2)}$, $C_3 = -\frac{2E}{r_i h^2(1+\mu)}$, $D_3 = \frac{E}{2r_i^3 k^2(1-\mu)}$, $E_3 = \frac{9E}{4r_i^2 h(1+\mu)}$, $F_3 = -\frac{9E}{2r_i^3(1+\mu)}$.

6 The application in curved rock

According to the shape and stress field characteristics of the curved strata, a schematic diagram of coal seam mining in the curved strata is set up as shown in Fig. 1. Here, the shape of the curved rock is simplified to a circular arc shape. The research object in this section is the overlying strata in the goaf, which is marked in red in Fig. 1.

6.1 Numerical calculation model

Figure 2 is a plane strain model for numerical calculation of curved strata. When the displacement function method is used to solve the computational model, the nodes in the computational domain should satisfy the governing equation for displacement function, and the boundary conditions should satisfy the boundary conditions as shown in Table 1. Special care has been taken to model the boundary conditions at the four corner nodes,

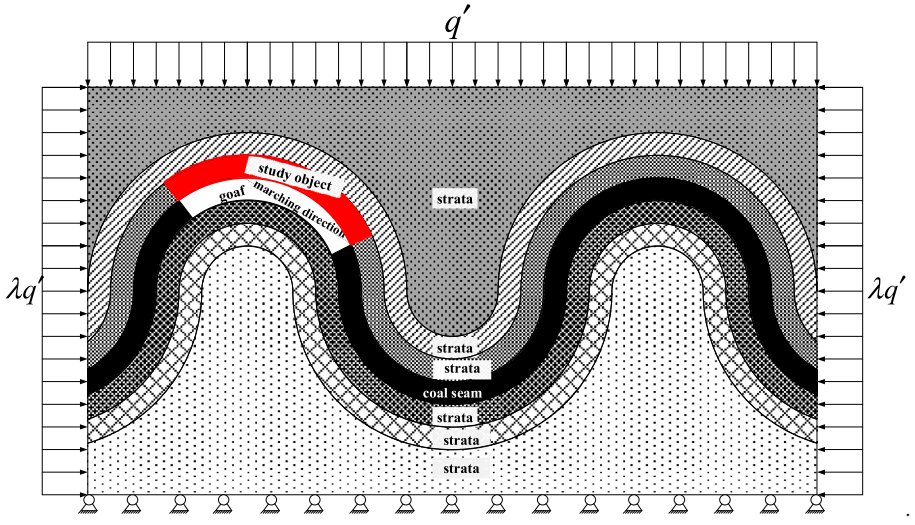

Figure 1 Schematic diagram of coal seam mining in curved rock

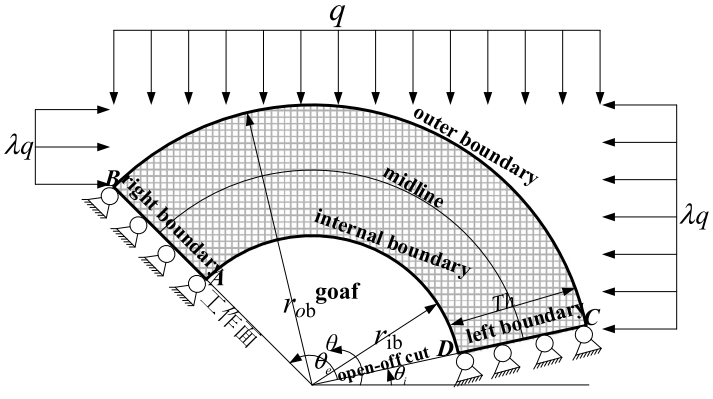

Figure 2 Numerical calculation model of curved strata

Table 1 Boundary conditions of the computational model

Boundary	Boundary conditions	
	Normal component	Tangential component
Right Boundary $\theta = \theta_l$	$u_r(r,\theta_l) = 0$	$u_\theta(r,\theta_l) = 0$
Left Boundary $\theta = \theta_{\max} = \theta_l + \theta_e$	$u_r(r,\theta_{\max}) = 0$	$u_\theta(r,\theta_{\max}) = 0$
Inner Boundary $r = r_{\mathrm{ib}}$	$\sigma_r(r_{\mathrm{ib}},\theta) = 0$	$\tau_{r\theta}(r_{\mathrm{ib}},\theta) = 0$
Out Boundary $r = r_{\mathrm{ob}}, \theta \le 90°$	$\sigma_r(r_{\mathrm{ob}},\theta) = -q(\lambda\cos\theta + \sin\theta)$	$\tau_{r\theta}(r_{\mathrm{ob}},\theta) = -q(\cos\theta - \lambda\sin\theta)$
Out Boundary $r = r_{\mathrm{ob}}, \theta > 90°$	$\sigma_r(r_{\mathrm{ob}},\theta) = -q(-\lambda\cos\theta + \sin\theta)$	$\tau_{r\theta}(r_{\mathrm{ob}},\theta) = -q(\cos\theta + \lambda\sin\theta)$

Table 2 Boundary conditions at four corners

Angular point	Given boundary conditions	Used boundary conditions	Boundary conditions of angular points
A	$\{u_r, u_\theta, \sigma_r, \tau_{r\theta}\}$	$\{u_r, u_\theta, \tau_{r\theta}\}$	$u_r = 0; u_\theta = 0; \tau_{r\theta} = 0$
B	$\{u_r, u_\theta, \sigma_r, \tau_{r\theta}\}$	$\{u_r, u_\theta, \tau_{r\theta}\}$	$u_r = 0; u_\theta = 0; \tau_{r\theta} = 0$
C	$\{u_r, u_\theta, \sigma_r, \tau_{r\theta}\}$	$\{u_r, u_\theta, \tau_{r\theta}\}$	$u_r = 0; u_\theta = 0; \tau_{r\theta} = 0$
D	$\{u_r, u_\theta, \sigma_r, \tau_{r\theta}\}$	$\{u_r, u_\theta, \tau_{r\theta}\}$	$u_r = 0; u_\theta = 0; \tau_{r\theta} = 0$

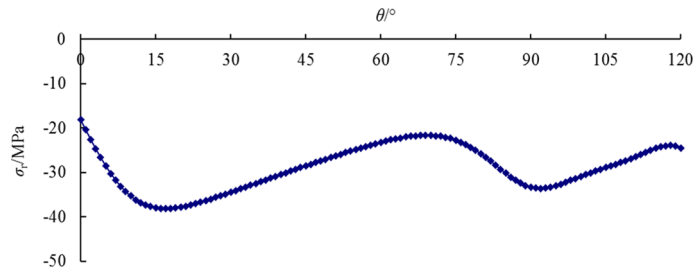

Figure 3 Distribution of radial stress along the middle circumference

the details of which are illustrated in Table 2. It can be seen from Table 2 that three out of the available four boundary conditions are satisfied at each corner nodes of the domain, and the remaining one is considered as redundant. It can be mentioned that usual computational approaches use two out of four conditions at each corner nodes to obtain the solution and thus the stresses around the corner regions deviate more from the actual stress state. Here, the mesh length h is 0.5 m and the mesh length k is 1°.

6.2 Stress analysis of curved strata

Taking inner radius r_{ib} = 20 m, the coefficient of tectonic stress λ = 1.8, mining depth md = 1000 m, advancing angle θ_e = 120°, mining location θ_i = 0°, and rock thickness st = 20 m as examples, the distribution characteristics of radial stress in the computational model are given as follows.

6.2.1 Distribution of radial stress in curved strata

Figure 3 presents the distribution of radial stress along the middle circumference in the computational model. It can be concluded that the radial stress is unevenly distributed along the middle circumference. The radial stress increases with the increase of angle θ in the range of 0°∼17°, decreases with the increase of angle θ in the range of 18°∼69°, increases with the increase of angle θ in the range of 70°∼92°, decreases with the increase of angle θ in the range of 93°∼120°, and the maximum value of radial stress is located

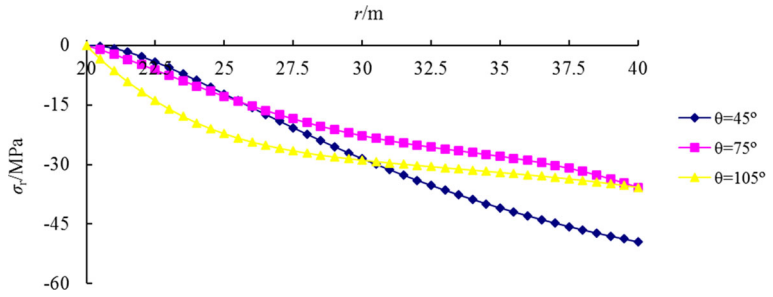

Figure 4 Distribution of radial stress for three different sections

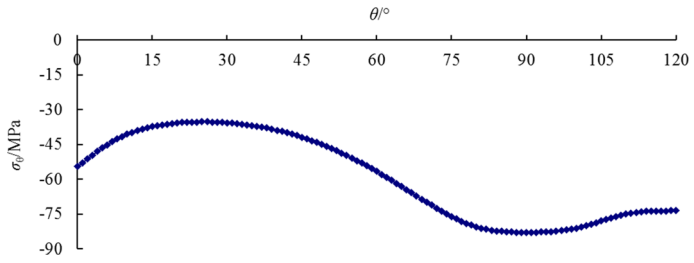

Figure 5 Distribution c of circumferential stress along the middle circumference

around $\theta = 15°$. It can be seen that the radial stress will reach a peak value not far from open-off cut. The distribution of radial stress for three different sections ($\theta = 45°$, $75°$ and $105°$) is shown in Fig. 4. The radial stress increases gradually from the inner surface to the outer surface along the radial direction, and the radial stress for $\theta = 45°$ increases faster comparing with the other two sections, which indicates that the radial stress increases faster for the section closer to open-off cut. On the contrary, the radial stress increases slow and the value of radial stress is small. It is worth mentioning that the radial stress values for all sections on the inner surface are zero, which indicate that the results conform to the boundary conditions of radial stress on the inner surface.

6.2.2 Distribution of circumferential stress in curved rock strata

Figure 5 presents the distribution of circumferential stress along the middle circumference in the computational model. It can be concluded that circumferential stress is unevenly distributed along the middle circumference. The circumferential stress decreases with the increase of angle θ in the range of $0°\sim25°$, the circumferential stress increases with the increase of angle θ in the range of $26°\sim90°$, the circumferential stress decreases with the increase of angle θ in the range of $91°\sim120°$, and the maximum value of circumferential stress is located around $\theta = 90°$. It can be seen that the circumferential stress will reach the peak value not far behind the working face. Therefore, more observations should be carried out behind the working face during the mining because the circumferential stress will easily cause the breaking along circumference. The distribution of circumferential stress for three different sections ($\theta = 45°$, $75°$ and $105°$) is shown in Fig. 6. It can be seen that the circumferential stress for $\theta < 90°$ increases from the inner surface to the outer surface along the radial direction, while the circumferential stress for $\theta > 90°$ decreases from the inner surface to the outer surface. For example, the value of circumference stress

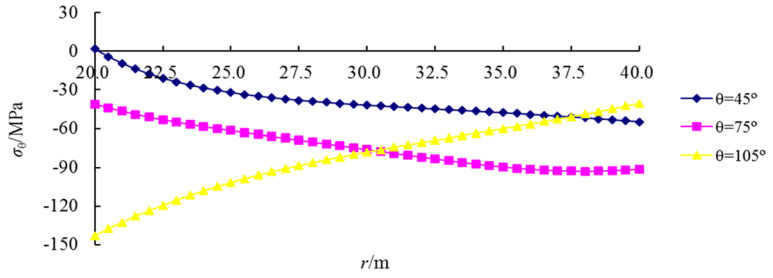

Figure 6 Distribution of circumferential stress for three different sections

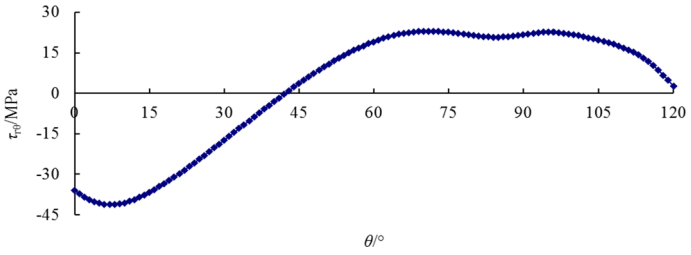

Figure 7 Distribution of shear stress along the middle circumference

for $\theta = 75°$ is 40.99 MPa on the inner surface, while the value is 91.28 MPa on the outer surface. The circumferential stress for $\theta = 105°$ decreases by about 70% from the inner surface to the outer surface. It should be mentioned that the value of circumferential stress for sections ($\theta = 75°\sim105°$) is larger than for other sections, which may easily cause the circumferential compression breaking in the overlying strata. Therefore, more observation should be carried out during the mining for these sections, and necessary measures should be taken for avoiding the disaster accidents.

6.2.3 Distribution of shear stress in curved strata

Figure 7 presents the distribution of shear stress along the middle circumference in the computational model. It can be concluded that the shear stress has both positive and negative values, and the distribution is also uneven along the middle circumference. The shear stress has negative values in the range of $0°\sim42°$, and the shear stress increases first and then decreases with the increase of angle θ in this range. The shear stress has positive values in the range of $43°\sim120°$, and the shear stress increases first and then decreases with the increase of angle θ in this range. The shear stress is relatively stable and does not change much in the range of $60°\sim105°$, but the maximum value of shear stress is located around $\theta = 10°$. It can be seen that the shear stress will reach the peak value not far from the open-off cut. The distribution of shear stress for three different sections ($\theta = 45°$, $75°$, and $105°$) is shown in Fig. 8. The shear stress for $\theta < 75°$ increases from the inner surface to the outer surface along the radial direction, while the shear stress for $\theta = 105°$ increases first and then decreases to negative values. It is worth mentioning that the shear stress values for all sections on the inner surface are zero, which indicates that the results conform to the boundary conditions of shear stress on the inner surface.

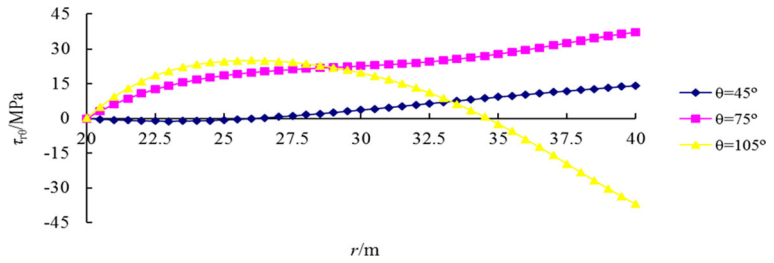

Figure 8 Distribution of shear stress for three different sections

7 Conclusions

In the present research, a modification to the usual approach of analyzing the plane curved beam with mixed boundary conditions in polar coordinates is introduced, which has been realized through the development of a displacement function based finite difference scheme. The novel of the present approach is that the governing equation for the plane problem is expressed in terms of a single partial differential equation. This method can handle mixed mode of boundary conditions, which is in contrast with the classical stress function formulation. Moreover, the finite difference scheme for governing equation, displacement components, and stress components has been developed, and the difference equations are also obtained in present paper. Finally, these theoretical formulations are applied to analyze the stress distribution of curved rock during the coal seam mining, which will provide scientific basis and reference for coal mining engineering.

Acknowledgements
The authors would like to thank the referees for careful reading and several constructive comments and for making some useful corrections that have improved the presentation of this paper.

Funding
Financial support for this work, provided by the National Fund for Nature projects (No. 51574228), the Research Foundation of Heze University (No. XY17KJ03) and Engagement Fund of Heze University (NO. XYPY02), the General Project of Science and Technology Plan of Shandong University (J17KB044), and General Items of Teaching Reform of Heze University (2016064), is gratefully acknowledged.

Availability of data and materials
This paper does not analyse or generate any datasets.

Competing interests
The authors declare that they have no competing interests.

Authors' contributions
The authors have achieved equal contributions. All authors read and approved the manuscript.

Publisher's Note

Received: 16 November 2018 Accepted: 4 April 2019 Published online: 15 April 2019

References

1. Timoshenko, S.P., Goodier, J.N.: Theory of Elasticity. Mc Graw-Hill Book Company, New York (1979)
2. Zhi-lun, X.: Mechanics of Elasticity. Higher Education Press, BeiJing (2002)
3. Mcclay, K.R., Price, N.J.: Thrust and Neppe Tectonics, pp. 9–544. Geological Social, London (1981)
4. Mcclay, K.R.: Thrust Tectonics. Chapman & Hall, London (1992) 447
5. Ding, H., Shu, C.: A stencil adaptive algorithm for finite difference solution of incompressible viscous flows. J. Comput. Phys. **214**(1), 397–420 (2006)
6. Min, C., Gibou, F., Ceniceros, H.D.: A supra-convergent finite difference scheme for the variable coefficient Poisson equation on non-graded grids. J. Comput. Phys. **218**(1), 123–140 (2006)

7. Bieniasz, L.K.: Experiments with a local adaptive grid h-refinement for the finite-difference solution of BVPs in singularly perturbed second-order ODEs. Appl. Math. Comput. **195**(1), 196–219 (2008)
8. Hossain, M.Z., Ahmed, S.R., Uddin, M.W.: Generalized mathematical model for the solution of mixed-boundary-value elastic problems. Appl. Math. Comput. **169**(2), 1247–1275 (2005)
9. Xu, W., Li, G.: Finite difference three-dimensional solution of stresses in adhesively bonded composite tubular joint subjected to torsion. Int. J. Adhes. Adhes. **30**(4), 191–199 (2010)
10. Nath, S.K.D., Ahmed, S.R.: A displacement potential-based numerical solution for orthotropic composite panels under end moment and shear loading. J. Mech. Mater. **4**(6), 987–1004 (2009)
11. Mc Corquodale, P., Colella, P., Grote, D.P., Vay, J.L., et al.: A node-centered local refinement algorithm for Poisson's equation in complex geometries. J. Comput. Phys. **201**(1), 34–60 (2004)
12. Li, Z.L., Dou, L.M., Cai, W., et al.: Investigation and analysis of the rock burst mechanism induced within fault-pillars. Int. J. Rock Mech. Min. Sci. **70**, 192–200 (2014)
13. Chen, X.H., Li, W.Q., Yan, X.Y.: Analysis on rock burst danger when fully-mechanized caving coal face passed fault with deep mining. Saf. Sci. **50**, 645–648 (2012)
14. Jiang, Y.D., Wang, T., Zhao, Y.X., et al.: Experimental study on the mechanisms of fault reactivation and coal bumps induced by mining. J. Coal Sci. Eng. **19**, 507–513 (2013)
15. Ji, H.G., Ma, H.S., Wang, J.A., et al.: Mining disturbance effect and mining arrangements analysis of near-fault mining in high tectonic stress region. Saf. Sci. **50**, 649–654 (2012)
16. Li, M., Zhang, J.X., Liu, Z., Zhao, X., Huang, P.: Mechanical analysis of roof stability under nonlinear compaction of solid backfill body. Int. J. Min. Sci. Technol. **26**(5), 863–868 (2016)
17. Li, Z.L., Dou, L.M., Cai, W., et al.: Investigation and analysis of the rock burst mechanism induced within fault-pillars. Int. J. Rock Mech. Min. Sci. **70**, 192–200 (2014)
18. Chen, X.H., Li, W.Q., Yan, X.Y.: Analysis on rock burst danger when fully-mechanized caving coal face passed fault with deep mining. Saf. Sci. **50**, 645–648 (2012)
19. Jiang, Y.D., Wang, T., Zhao, Y.X., et al.: Experimental study on the mechanisms of fault reactivation and coal bumps induced by mining. J. Coal. Sci. Eng. **19**, 507–513 (2013)
20. Cook, R.D.: Axisymmetric finite element analysis for pure moment loading of curved beams and pipe bends. Comput. Struct. **33**(2), 483–487 (1989)
21. Rattanawangcharoen, N., Bai, H., Shah, A.H.: A 3D cylindrical finite element model for thick curved beam stress analysis. Int. J. Numer. Methods Eng. **59**(4), 511–531 (2004)
22. Richards, T.H., Daniels, M.J.: Enhancing finite element surface stress predictions: a semi-analytic technique for axisymmetric solids. J. Strain Anal. Eng. Des. **22**(2), 75–86 (1987)
23. Smart, J.: On the determination of boundary stresses in finite elements. J. Strain Anal. Eng. Des. **22**(2), 87–96 (1987)
24. Gangan, P.: The curved beam/deep arch/finite ring element revisited. Int. J. Numer. Methods Eng. **21**(3), 389–407 (1985)
25. Dow, J.O., Jones, M.S., Harwood, S.A.: A new approach to boundary modeling for finite difference applications in solid mechanics. Int. J. Numer. Methods Eng. **30**(1), 99–113 (1990)
26. Ranzi, G., Gara, F., Leoni, G., Bradford, M.A.: Analysis of composite beams with partial shear interaction using available modeling techniques: a comparative study. Comput. Struct. **84**(13–14), 930–941 (2006)
27. Ahmed, S.R., Hossain, M.Z., Uddin, M.W.: A general mathematical formulation for finite-difference solution of mixed-boundary-value problems of anisotropic materials. Comput. Struct. **83**(1), 35–51 (2005)